

# THERMAL AND KINETIC STUDY OF THE FERROELECTRIC PHASE TRANSITION IN DEUTERATED TRIGLYCINE SELENATE

F. J. Romero<sup>1\*</sup>, M. C. Gallardo<sup>1</sup>, A. Czarnecka<sup>2</sup>, M. Koralewski<sup>2</sup> and J. del Cerro<sup>1</sup>

<sup>1</sup>Departamento de Física de la Materia Condensada, Instituto Mixto de Ciencia de Materiales CSIC-Universidad de Sevilla  
Apartado 1065, 41080 Sevilla, Spain

<sup>2</sup>Institute of Physics, Adam Mickiewicz University, Umultowska 85, 61-614 Poznań, Poland

The specific heat and the enthalpy variation of a highly deuterated crystal of ferroelectric triglycine selenate have been measured around its first-order phase transition using the technique square modulated differential thermal analysis (SMDTA). The low temperature variation rate has allowed analyzing the kinetics of the phase transition. Due to an internal crack in the sample, the transition is carried out in two steps and an intermediate region where the transition is blocked and both phases coexist without transformation has been found. The latent heat on cooling ( $L_c=1.32\pm0.02 \text{ J g}^{-1}$ ) is higher than on heating ( $L_h=1.08\pm0.02 \text{ J g}^{-1}$ ) due to the thermal hysteresis and the great difference between the specific heat in both phases. Nevertheless, the enthalpy balance is fulfilled on heating and on cooling.

**Keywords:** DTGSe, latent heat, metastable state, SMDTA, specific heat

## Introduction

The study of the thermal properties of a first-order phase transition whose specific heat shows an important anomaly presents some difficulties since the change of enthalpy includes the contribution from the latent heat  $L$  and the contribution due to the temperature dependence of the specific heat  $c$  around the transition temperature. Furthermore, the latent heat usually spreads over a certain temperature interval as a consequence of temperature gradients, internal stresses and defects and the specific heat data obtained in that temperature range are not valid.

When the contribution due to the heat capacity is small enough, the conventional techniques such as DTA or DSC allow evaluating the latent heat accurately. In other cases, the starting and ending points of the latent heat effect merge with the increase of  $c$  near the transition and it is difficult to determine the temperature interval where the effect of the latent heat is present and, consequently, to choose the appropriate baseline to determine  $L$ .

Temperature modulated differential scanning calorimetry (TMDSC) [1–4] tries to solve this problem; this technique is a conventional DSC where the temperature ramp is modulated by an alternative component (ACC). By means of a direct Fourier transform algorithm the continuous component (DSC) and the alternative component (ACC) are analysed separately. As a kinetic process affects in a different way

to DSC and ACC components, the comparison of both components allows discriminating the temperature range where the kinetic process, such a first order phase transition, is present. TMDSC technique has been improved during last years including sawtooth modulation [5, 6] and its precision in the measurement of heat capacities [7] has been investigated. A detailed discussion of its features and future prospects has been reported [8].

On the other hand, our group has developed an original method [9, 10], named square modulated differential thermal analysis (SMDTA) and based on conduction calorimetry, to investigate the first-order character of a phase transition and to evaluate the latent heat. A serial of long-periodic square thermal pulses is superposed to a heating or cooling ramp, whose temperature variation rate is extremely low, even lower than  $0.1 \text{ K h}^{-1}$ . The samples passes from a uniform temperature distribution to another one and the integration of the electromotive force (emf)  $V$ , given by two heat fluxmeters between both temperature distributions, allows to determine absolute values of the specific heat  $c$  of the sample [9] and to discriminate the temperature interval where the effect of the latent heat is produced.

The high number of thermocouples forming the fluxmeters allows the device to work at a very small temperature scanning rate ( $0.1 \text{ K h}^{-1}$ ). We can carry out a second run with the same temperature ramp but without modulation where the heat flux  $\phi_D$  exchanged

\* Author for correspondence: ffromero@us.es

between the sample and the calorimetric block, proportional to the electromotive force given by the fluxmeters, is measured. The comparison between  $\phi_D$  and the heat flux calculated from the specific heat data allows us to evaluate the latent heat even when the specific heat anomaly is very strong [11].

Due to the extremely low temperature scanning rate, the transformation from one phase to another takes place in a long period of time (generally more than one hour) and information about the kinetics of the phase transition is also obtained.

This technique has been successfully applied to study the almost tricritical phase transition in  $KMn_{1-x}Ca_xF_3$  whose ferroelastic phase transition shifts from first to second order when the Ca doping increases ( $L(x=0)=0.129 \text{ J g}^{-1}$  [11],  $L(x=0.5\%)=0.010 \text{ J g}^{-1}$  [12]). The influence of the uniaxial stress on the kinetics and on the domain growth of the ferro-paraelectric phase transition in  $KMnF_3$  has been obtained [13]. The technique has also been applied to show that the paramagnetic–antiferromagnetic phase transition of  $CoO$ , whose nature was controversial, is continuous [14] and to evaluate the critical field for the paraelectric–ferroelectric phase transition in KDP by measuring the effect of the electric field on its latent heat [15].

The above works correspond to studies of phase transitions close to the tricritical point so that the latent heat is relatively small. The aim of this paper is to apply this technique to a first-order phase transition whose latent heat is an order of magnitude higher than those previously studied and which shows a strong anomaly in the specific heat.

Pure triglycine selenate  $[(NH_2CH_2COOH)_3H_2SeO_4]$ , here-after TGSe, is a well-known uniaxial ferroelectric which undergoes a typical order–disorder phase transition at about  $T \sim 22^\circ C$  [16, 17]. In a recent paper [18], we analysed the phase transition of a high-purity sample of TGSe using SMDTA technique. No latent heat was found and the specific heat of the ferroelectric phase was found to follow a classical tricritical Landau potential. When TGSe is partially deuterated (DTGSe), dielectric susceptibility shows thermal hysteresis which increases when the deuteration increases [19–21], suggesting that the transition becomes first-order. Unfortunately, the deuteration also increases the fragility of the sample, producing cracks in the samples.

In this paper, we perform a thermal study of a DTGSe crystal (90% deuteration) but with an appreciable internal crack which cross the sample. We have measured, on cooling and heating, the temperature dependence of the specific heat and the influence of the thermal hysteresis on the latent heat. The influence of the crack on the kinetics of the phase transition is discussed.

## Experimental

### Characteristics of the sample

The sample of  $(TGSe)_{1-x}(DTGSe)_x$  was prepared at the Institute of Physics, Adam Mickiewicz University, Poznan (Poland). It was grown from aqueous solution by slow evaporation of water at constant temperature equal  $T_g=302 \text{ K}$ . The crystal obtained was colourless and of high optical quality. The degree of deuteration was estimated to be 90% from the relation given by Gesi [19]. The dielectric constant value at  $T_c$  was  $\epsilon_{max}=7000$  and 4500 on cooling and heating respectively (frequency  $\sim 1 \text{ kHz}$ ). The ferroelectric axis,  $b$ -axis, of the single crystal was determined by the cleavage plane (010). The main faces, which had a pseudo-hexagonal cross section with an area of  $55 \text{ mm}^2$ , were prepared perpendicular to the  $b$ -axis and gold electrodes were evaporated on them. The thickness of the sample was 2.55 mm and the mass  $m=0.35 \text{ g}$ . An internal crack was observed in the sample.

### Description of the calorimeter

The experimental arrangement has been described in detail [22] and it is represented in Fig. 1. The sample is pressed between two identical heat fluxmeters, which are made from 50 chromel-constantan thermocouples [23] connected in series with the wires placed in parallel lines. One of the fluxmeters is fixed to a calorimeter block while the other is pressed by a bellows, which allows applying uniaxial stress to the sample. The fluxmeters, which have a cross section of  $1 \text{ cm}^2$ , are rigid enough to apply a controlled uniaxial stress on the sample in the range between 0 and 12 bar. Two electrical resistances (heaters) are placed between each face of the sample and fluxmeters. These resistances can dissipate a uniform heat power on the sample face. Sensors and heaters are placed in a cylindrical hole made in a cylindrical piece of bronze (10 kg) which serves as the heat sink (the calorimeter block). The block and two surrounding radiation shields are placed into a hermetic outer case un-

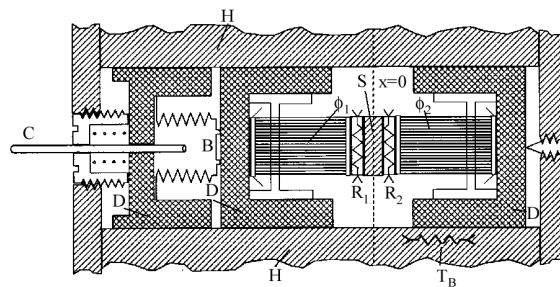


**Fig. 1** Diagram of the sensor:  $\phi_1$  and  $\phi_2$  – heat fluxmeters,  $R_1$  and  $R_2$ , heaters,  $S$  – sample,  $B$  – bellow,  $D$  – fluxmeter and bellow container,  $H$  – heat sink,  $C$  – capillary

der vacuum ( $10^{-7}$  torr). The entire assembly is placed in a Dewar jar filled with liquid refrigerant whose temperature is controlled by a close-cycle circulation provided by a thermostat (Julabo FP40), which is able to establish very low temperature variation rates. The high vacuum inside the outer case, the radiation shields and the high thermal capacity of the block assure the thermal stability in the sample and it allows to carry out the measurement on quasistatic conditions changing the temperature of the block at a very low constant rate ( $dT/dt < 0.1 \text{ K h}^{-1}$ ).

Due to the high thermal inertia of the equipment, the starting temperature of the experiment is selected several degrees higher (on cooling) or lower (on heating) than the interval of temperatures under study to allow the equipment reach the desired temperature scanning rate set in the thermostat.

A HPE-1328A current source and HPE-1326 multimeter are used respectively to produce and to measure the power dissipated in the heaters. The electromotive force (emf) produced by the fluxmeters is measured by a Keithley 2182 nanovoltmeter. All the devices are controlled by a HP-75000 data acquisition system.

#### *Specific heat measurements*

##### *Measurement method*

Let us consider now that the temperature of the calorimeter is changing continuously in time at a rate of about  $0.1 \text{ K h}^{-1}$ . In the simplest case, the temperature gradient along the calorimeter is constant and a quantity of heat (necessary for changing the temperature of the sample) will be flowing through the fluxmeter giving a small but non-zero electromotive force  $V_0$ .

Under this circumstance the specific heat of the sample is measured by superposing a serial of square thermal pulses of amplitude  $\Delta T$  and period  $2\tau$ . At  $t=t_0$  a constant power  $W_0$  is dissipated in both heaters for a time  $\tau$  which allows the sample reach a new steady-state temperature distribution. At time  $t=t_0+\tau$  the power  $W_0$  will flow through the fluxmeters, which will give a proportional electromotive force  $V_1$ . Let us call  $\Delta T$  the temperature increase at the edges of the sample between  $t_0$  and  $t_1$ . At this time  $t=t_1$ , the power  $W_0$  is cut off and the sample relaxes to the initial temperature distribution at time  $t_2=t_1+2\tau$ , when the power  $W_0$  is dissipated again and the process is continuously repeated.

We measure the specific heat [9] by integrating the transient response  $V(t)$  between  $t_0$  and  $t_1$  or between  $t_1$  and  $t_2$ . Two different quantities can be considered: the integral obtained while the heaters are dissipating (dissipation branch) and the integral obtained while there is no dissipation (relaxation branch). Correspondingly, we obtain two values of

the specific heat, that on the dissipating branch,  $c_d$ , and on the relaxation branch,  $c_r$ .

In this experiment, the temperature variation rate was  $0.03 \text{ K h}^{-1}$ . Taking into account the semiperiod of the pulse signal,  $\tau=12 \text{ min}$ , the change of temperature during the measurement of  $c_d$  or  $c_r$  due to the ramp is about  $\Delta T_\tau=0.005 \text{ K}$ . The increase of temperature  $\Delta T$  due to the heat dissipated on the heaters during the dissipation branch is evaluated to be about  $0.01 \text{ K}$ .

According to this, during the relaxation branch when cooling and dissipation branch when heating  $\Delta T$  and  $\Delta T_\tau$  have the same sign (positive superposition). During relaxation branch when heating and dissipation branch when cooling  $\Delta T$  and  $\Delta T_\tau$  have opposite sign (opposite superposition) and the temperature variation of the sample is reversed because  $\Delta T > \Delta T_\tau$ .

When there is not any kinetic effect, relaxation branch and dissipation branch are equivalent on both heating and cooling ramps. Under these conditions,  $c_d$  and  $c_r$  data match.

When a kinetic process such as a first order phase transition takes place, in the temperature interval where the latent heat effect is present, relaxation branch and dissipation branch are not equivalent due, between other reasons, to the thermal hysteresis. In this case,  $c_d$  and  $c_r$  do not coincide and they show a non-regular behaviour due to the effect of the latent heat. This fact allows us to discriminate the temperature interval where the first-order phase transition takes place [10].

##### *Specific heat results*

In Fig. 2 we represent a typical curve for the specific heat of DTGSe (90% deuteration) vs. temperature in a range of 35 K around the transition temperature. The specific heat shows a very important anomaly around 306 K. To analyse in detail the behaviour near the transition temperature and the thermal hysteresis, we plot  $c_d$  and  $c_r$  in a smaller temperature interval around the transition temperature on cooling (Fig. 3a) and on heating (Fig. 3b). We have also represented the periodical electromotive force  $V$  (transient response) given by the fluxmeters vs. time during the specific heat measurement process on cooling (Fig. 4a) and on heating (Fig. 4b). In each graph, we can distinguish five regions which have been labelled from A to E. In each region the behaviour is very similar on cooling and on heating although the temperatures which limit each one are slightly different as a consequence of the thermal hysteresis and the different kinetics of both processes.

In regions A, C and E  $c_d$  and  $c_r$  show the same behaviour (Figs 3a and b) and no anomaly is found in the transient response  $V$  (Figs 4a and b). It indicates that there is not effect from the latent heat in these re-

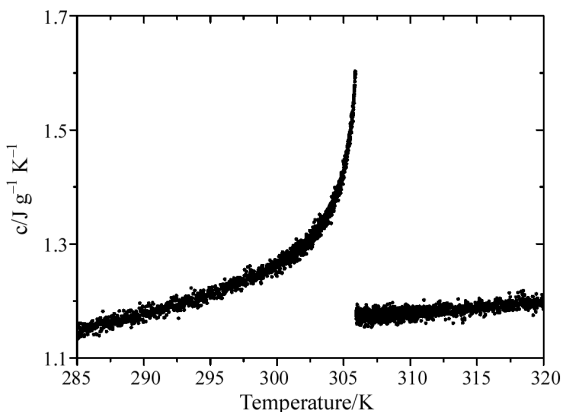


**Fig. 2** Typical curve of specific heat for a 90% deuterated TGSe sample at  $0.03 \text{ K h}^{-1}$

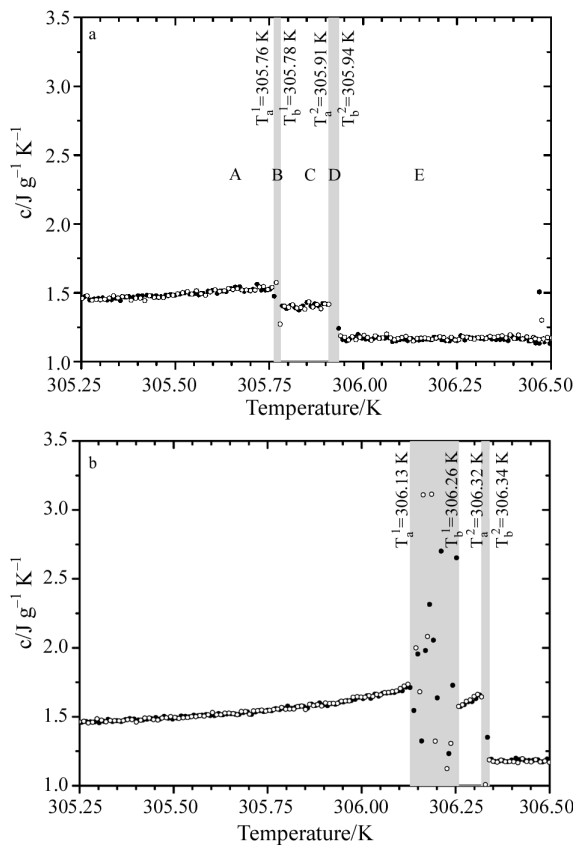


**Fig. 3** Specific heat for the dissipation branch,  $\bullet - c_d$  and for the relaxation branch,  $\circ - c_r$  on a – cooling and b – heating

gions. Region A and E corresponds respectively to the interval where the sample is completely in the ferroelectric phase and in the paraelectric phase.

On heating and cooling, in regions B and D,  $c_d$  and  $c_r$  data do not coincide and show very anomalous values which are even out of scale in the figures. According with the previously reported method [10], it indicates that the phase transformation takes place in both regions. This fact is confirmed by the periodical

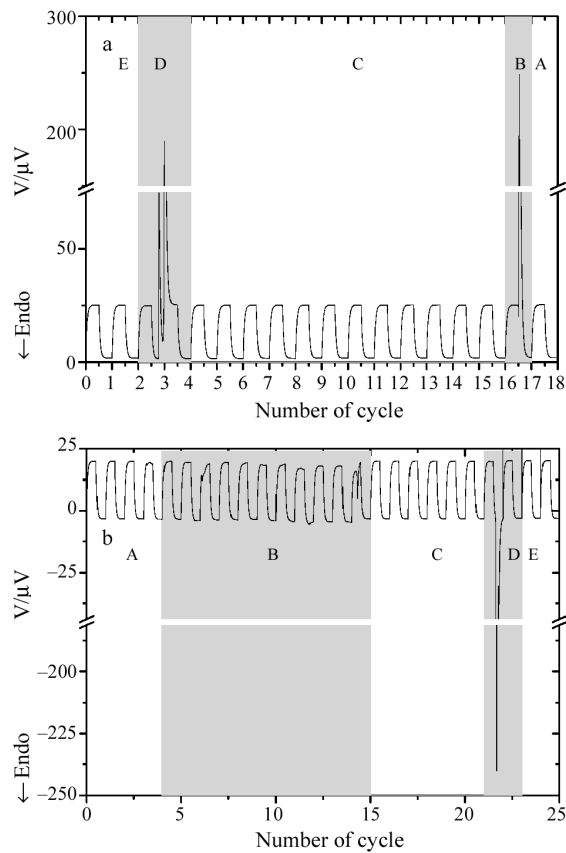


**Fig. 4** Transient response for the electromotive force  $V$  during the specific heat measurements on a – cooling and b – heating

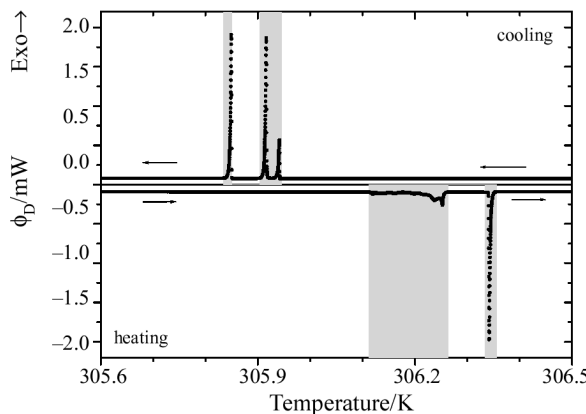
response given by the fluxmeter during the specific heat measurements. In region D, strong peaks are clearly observed in  $V$  indicating a very sharp thermal effect due to an abrupt change of phase. In region B, we observe that  $V$  presents two sharp peaks on cooling while a lot of small anomalies appear on heating. This different behaviour is attributed to a different kinetics for both processes.

The behaviour of the sample in region C will be discussed below.

#### Heat flux measurements

We have carried out a second experiment where the temperature of the sample changes at  $0.1 \text{ K h}^{-1}$  but without the periodical dissipation in the heaters. The heat flux  $\phi_D$  exchanged between the sample and the calorimeter block has been measured every 5 s (this interval between the data is imposed by the time that it is necessary to get a precise measurement of the temperature).

In Fig. 5, we represent  $\phi_D$  vs. temperature on cooling and on heating around the transition temperature. We observe the same behaviour found in the analysis of the periodical response in Fig. 4. On cooling three peaks are clearly observed while on heating

**Fig. 5** DTA trace  $\phi_D$  on heating and cooling at  $0.1 \text{ K h}^{-1}$ 

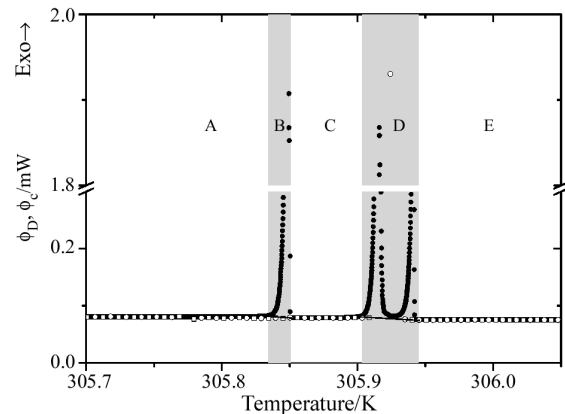
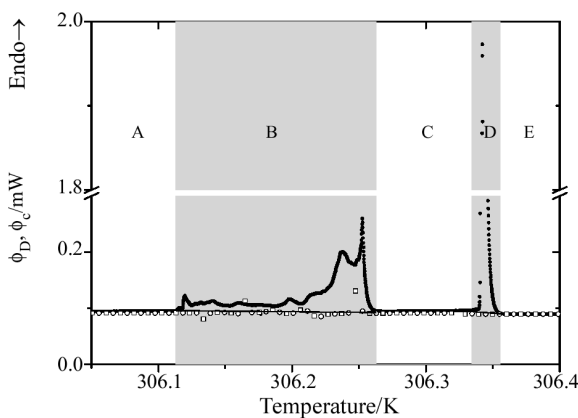
there are two peaks, one of them close to a serial of small overlapping anomalies. The thermal hysteresis is estimated to be 0.18 K.

Data in Fig. 5 have been zoomed in Figs 6 and 7 on cooling and heating, respectively.

On the other hand, using the specific heat data represented in Fig. 3 and following the procedure described in [11], we calculate the heat flux  $\phi_c$  which would correspond exclusively to the heat capacity contribution. Since  $\phi_D$  and  $\phi_c$  are obtained with the same device, on the same sample and under similar thermal conditions, it is possible to compare them. The latent heat or whatever kinetic process is present in the temperature interval ( $T_1, T_2$ ) where  $\phi_D$  and  $\phi_c$  do not coincide. The latent heat is determined by integrating the DTA trace  $\phi_D$  in that interval and using the straight line  $\phi_D(T_1) - \phi_D(T_2)$  as baseline. Obviously, when both coincide, the transition is considered to be second order.

In Figs 6 and 7, we have also represented the calculated heat flux  $\phi_c$  [11]. We can distinguish the five regions previously reported in the specific heat analysis. On heating and on cooling  $\phi_D$  and  $\phi_c$  coincide in regions A, C and E. This confirms the previously statement that in region C there is not any effect from the latent heat. This effect is present in regions B and D, where  $\phi_D$  and  $\phi_c$  clearly do not coincide. The limits of these regions do not coincide exactly in Figs 3, 6 and 7. They are shifted in some hundredth of degree and the temperature interval where the transition is entirely completed in the specific heat measurements is 0.05 K lower than in the case of heat flux measurements. It is reasonable to assume that those differences are due to the different kinetics of the change of phase in both experiments.

In spite of these small differences, it is clearly found that the heat flux in regions A, C and E is due to the change of enthalpy produced by the temperature dependence of the specific heat. The facts that in region C  $\phi_D = \phi_c$  and  $c_d = c_r$  suggest that the effect of the

**Fig. 6** Experimental DTA trace  $\phi_D$  on ● – cooling and DTA trace calculated from the specific heat measurements ○ –  $\phi_c$  from  $c_r$  and □ –  $\phi_c$  from  $c_d$ . The baseline used to calculate the latent heat is also included**Fig. 7** Experimental DTA trace ● –  $\phi_D$  on heating and DTA trace calculated from the specific heat measurements ○ –  $\phi_c$  from  $c_r$  and □ –  $\phi_c$  from  $c_d$ . The baseline used to calculate the latent heat is also included

latent heat is only present in regions B and D in Figs 6 and 7. All these facts indicate that the transition is carried out in two stages at temperatures which differ in about 0.1 or 0.07 K when cooling or heating. This cannot be attributed to a non-uniform deuteration in the sample because in this case the phase transition anomaly would be broadened, spreading the latent heat effect over a larger temperature interval. It is reasonable to assume that the transition is partially blocked by the crack present in the sample. According to this, in region C both phases coexist in a metastable state keeping constant the molar fraction of each one. The transition is completed in regions B and D when cooling or when heating respectively. We must point out that the heat flux peak is extremely abrupt in these regions as a consequence of a sudden change of phase due to the metastable situation of the crystal. In these regions the abrupt change of phase produces specific heat data which are out of scale in Fig. 3.

**Table 1** Contributions from each region (as labelled in the text) to enthalpy difference between a state in the paraelectric phase at 306.5 K and a state in the ferroelectric phase at 305.5 K. The uncertainty in each contribution variation is estimated to be lower than 5 mJ g<sup>-1</sup>

Region	$\Delta H$ cooling/J g <sup>-1</sup>	$\Delta H$ heating/J g <sup>-1</sup>
A	0.120	0.234
B	0.535	0.552
C	0.029	0.052
D	0.784	0.633
total	1.468	1.471

The latent heat is evaluated by integrating  $\phi_D$  with respect to the baseline shown in Figs 6 and 7. The contributions to the latent heat corresponding to regions B and D are, respectively,  $0.54 \pm 0.01$  and  $0.78 \pm 0.01$  J g<sup>-1</sup> on cooling and  $0.45 \pm 0.01$  and  $0.63 \pm 0.01$  J g<sup>-1</sup> on heating. The proportion between both contributions shows that, due to the crack in the sample, the transition is blocked during a temperature interval of 0.1 K (1 h) on cooling (0.07 K on heating) with a proportion of 59% of the sample in the ferroelectric phase.

The latent heat is evaluated to be  $L_c = 1.32 \pm 0.02$  J g<sup>-1</sup> on cooling and  $L_h = 1.08 \pm 0.02$  J g<sup>-1</sup> on heating. Some difference between the latent heat on cooling and heating is expected as a consequence of the thermal hysteresis because the specific heat on heating reaches values higher than on cooling and, therefore, contributes more significantly to the enthalpy.

Nevertheless, the balance of enthalpy must be satisfied. To check this statement, we have calculated the enthalpy difference between a state in the paraelectric phase (306.5 K), which is taken as the reference, and a state in the ferroelectric phase

(305.6 K) from the integration of the heat flux measurements for cooling and heating runs (Fig. 8). The values corresponding to each region have been listed in Table 1. The integration of the heat flux includes the contribution from the latent heat and the contribution from the specific heat variation with the temperature in each region. It is observed that, in spite of the different kinetics of both transformations and the different magnitude of the steps due to latent heat contributions, the enthalpy balance is fulfilled.

## Conclusions

The application of SMDTA technique to the thermal study of the phase transition in DTGSe crystal (90% deuteration) has confirmed the advantages of this method. It allows the measurement of absolute values of specific heat and latent heat and the determination of the temperature interval where a first-order phase transition or whatever kinetic process takes place, even in the case that the specific heat varies strongly around the transition temperature.

The high sensitivity of the equipment allows us to use an extremely low scanning temperature range, so that information about the kinetics of the transformation from one phase to another is obtained. Taking into account a temperature variation rate of 0.1 K h<sup>-1</sup> and the width of the heat flux peaks shown in Figs 5 and 6, we obtain that these peaks take a time similar to the relaxation time of the fluxmeter (12 min). Consequently, those peaks correspond to very abrupt partial changes of phase. This suggests that on cooling, the formation of ferroelectric domains has been carried out in three different steps: two former abrupt changes partially overlapped which transform the 59% of the sample to the ferroelectric phase. Then the transition is blocked during an interval of 0.12 K when finally the rest of the sample changes suddenly to the ferroelectric phase. On heating we observe that the transition to the paraelectric phase begins with a serial of small overlapped peaks indicating a gradual disappearance of the ferroelectric phase. When 41% of the sample is transformed, the transition is blocked during an interval of 0.07 K and finally the transition is abruptly completed.

## Acknowledgements

This work has been supported by Project BFM2002-02237 of the Spanish DGICYT.

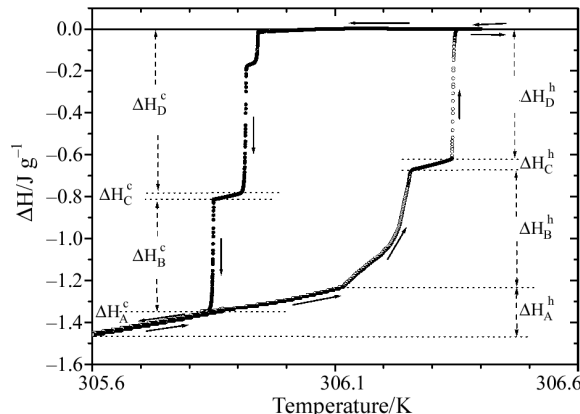


**Fig. 8** Enthalpy variation between a state in the paraelectric phase (306.5 K) and a state in the ferroelectric phase (305.6 K) on ● – cooling and ○ – heating. The contributions from the different regions (the superscript in  $\Delta H$  indicates the cooling or heating run and the subscript indicates the region) are indicated in the figure and the values are listed in Table 1

## References

- 1 P. S. Gill, S. R. Sauerbrunn and M. Reading, *J. Thermal Anal.*, 39 (1993) 931.
- 2 M. Reading, D. Elliot and V. L . Hill, *J. Thermal Anal.*, 40 (1993) 949.
- 3 I. Hatta, H. Ichikawa and M. Todoki, *Thermochim. Acta*, 267 (1995) 83.
- 4 I. Hatta and S. Nakayama, *Thermochim. Acta*, 318 (1998) 21.
- 5 B. Wunderlich, *J. Thermal Anal.*, 48 (1997) 207.
- 6 W. Hu and B. Wunderlich, *J. Therm. Anal. Cal.*, 66 (2001) 677.
- 7 J. Pak, W. Qiu, M. Pyda, E. Nowak-Pyda and B. Wunderlich, *J. Therm. Anal. Cal.*, 82 (2005) 565.
- 8 B. Wunderlich, *J. Therm. Anal. Cal.*, 78 (2004) 7.
- 9 J. del Cerro, *J. Thermal Anal.*, 34 (1988) 335.
- 10 J. del Cerro, J. M. Martín-Olalla and F. J. Romero, *Thermochim. Acta*, 401 (2003) 149.
- 11 J. del Cerro, F. J. Romero, M. C. Gallardo, S. A. Hayward and J. Jiménez, *Thermochim. Acta*, 343 (2000) 89.
- 12 F. J. Romero, M. C. Gallardo, J. Jiménez and J. del Cerro, *Thermochim. Acta*, 372 (2001) 25.
- 13 F. J. Romero, M. C. Gallardo, J. Jiménez, J. del Cerro and E. K. H. Salje, *J. Phys.: Condens. Matter*, 12 (2000) 4567.
- 14 F. J. Romero, J. Jiménez and J. del Cerro, *J. Magn. Magn. Mater.*, 280 (2004) 257.
- 15 J. M. Delgado-Sánchez, J. M. Martín-Olalla, M. C. Gallardo, S. Ramos, M. Koralewski and J. del Cerro, *J. Phys.: Condens. Matter*, 17 (2005) 2645.
- 16 F. Jona and G. Shirane, *Ferroelectric crystals*, Pergamon, New York 1962.
- 17 B. T. Matthias, C. E. Miller and J. Remeika, *Phys. Rev.*, 104 (1956) 849.
- 18 F. J. Romero, M. C. Gallardo, J. Jiménez, M. Koralewski, A. Czarnecka and J. del Cerro, *J. Phys.: Condens. Matter*, 16 (2004) 7637.
- 19 K. Gesi, *J. Phys. Soc. Jpn.*, 41 (1976) 565.
- 20 C. Aragó and J. A. Gonzalo, *J. Phys.: Condens. Matter*, 12 (2000) 3737.
- 21 C. Aragó and J. A. Gonzalo, *Ferroelectr. Lett.*, 27 (2000) 83.
- 22 M. C. Gallardo, J. Jiménez and J. del Cerro, *Rev. Sci. Instrum.*, 66 (1995) 5288.
- 23 J. Jiménez, E. Rojas and M. Zamora, *J. Appl. Phys.*, 56 (1984) 3353.

Received: November 21, 2005

Accepted: March 10, 2006

OnlineFirst: September 15, 2006

DOI: 10.1007/s10973-005-7444-7